

Hydrogen in anion vacancies of semiconductors

Mao-Hua Du and David J. Singh

Materials Science and Technology Division and Center for Radiation Detection Materials and Systems, Oak Ridge National Laboratory, Oak Ridge, Tennessee 37831, USA

(Received 16 December 2008; revised manuscript received 8 April 2009; published 6 May 2009)

Density-functional calculations show that, depending on the anion size, hydrogen in anion vacancies of various II-VI semiconductors can be either twofold or fourfold coordinated and has either amphoteric or shallow donor character. In general, the multicoordination of hydrogen in an anion vacancy is the indication of an anionic H, H^- ion, in the relatively ionic environment. In more covalent semiconductors, H would form a single cation-H bond in the anion vacancy.

DOI: [10.1103/PhysRevB.79.205201](https://doi.org/10.1103/PhysRevB.79.205201)

PACS number(s): 61.72.J-, 61.72.S-, 71.55.Gs

I. INTRODUCTION

Hydrogen is an important impurity in many semiconductors. It can passivate electrically active impurities and defects. It can also provide conductivity directly by acting as a shallow donor¹ or indirectly as a codopant by boosting the concentration of other shallow dopants.^{2,3} The interaction between hydrogen and vacancies in semiconductors has been extensively studied for decades. Typically, hydrogen can terminate the dangling bonds around a vacancy, thereby partially or completely passivating the vacancy. However, it has been shown recently by density-functional calculations that hydrogen in anion vacancies (V_{anion}) of many semiconductors, such as ZnO,⁴ MgO,⁴ InN,⁵ SnO₂,⁶ and GaN,⁷ acts as an unintentional shallow donor, providing *n*-type conductivity to the materials. Furthermore, the hydrogen is found to be located near the center of the vacancy and coordinated to multiple nearest-neighbor cations.

The multicoordination of the hydrogen in anion vacancies has led to discussion of the nature of chemical bonding around the hydrogen.^{4,8} A multicenter covalent bonding model was initially proposed.^{4,5} However, the electronic structural analyses showed that the hydrogen in the O vacancy of ZnO is anionic, i.e., the H^- ion.⁸ The H^- configuration is stabilized by the ionic bonding with the host ionic matrix rather than by the multicenter covalent bond. The single-electron donor character of $V_{\text{O}}\text{-H}$ is simply the result of replacing the O^{2-} ion with the H^- ion.

In the ionic crystals, hydrogen is known to exist as H^- ions in anion vacancies, e.g., the *U* center in alkali halides.⁹⁻¹¹ It may be noted that the multicoordination of H found in recent calculations all exists in crystals of relatively high ionicity, e.g., ZnO, MgO, InN, SnO₂, and GaN. This may be explained by the fact that H is stabilized by the Ewald field of the ionic matrix and thus its coordination number is not constrained by the number of available electron pairs, which is only essential for the bonding in covalent materials.

Driven by the Coulomb attraction, H^- would approach the cation as close as possible until the electronic shell overlap between the cation and H^- is large enough to cause repulsion. It may thus be expected that H^- would stay in the center of the anion vacancy if the anion size is small and the cation size is big but would move off center if the anion size

becomes large. We show by density-functional calculations that, in ZnX ($X=\text{S, Se, and Te}$) and CdX ($X=\text{S and Te}$), indeed, H moves off center but remains in the multicoordinated structure (i.e., twofold coordination). The calculated H local vibration modes (LVMS) are in good agreement with the experimental results, thus supporting the proposed H structures. H in anion vacancies is found to be amphoteric in all the II-VI semiconductors we have studied except the oxides.

II. METHOD

We performed calculations based on density-functional theory within the local-density approximation (LDA), as implemented in VASP.¹² The electron-ion interactions are described by projector augmented wave pseudopotentials.¹³ The valence wave functions are expanded in a plane-wave basis with cutoff energy of 400 eV. All the calculations were performed using 64-atom cubic cells. A $2 \times 2 \times 2$ grid was used for the *k*-point sampling of Brillouin zone. All the atoms were relaxed to minimize the Feynman-Hellmann forces to below 0.02 eV/Å. We used zinc-blende structures for all the semiconductors under study. The calculated lattice constants of these materials are compared with the experimental results in Table I. The methods for calculating the transition energy levels can be found in Ref. 14.

III. RESULTS

We have considered all the possible coordination numbers for the hydrogen in the anion vacancies of the semiconduc-

TABLE I. The LDA lattice constants compared with the experimental values at room temperature (in Ref. 28). The zinc-blende structure is adopted for all the semiconductors listed in this table. All units are in Å.

| | LDA | Expt. |
|------|-------|--------|
| ZnO | 4.510 | 4.63 |
| ZnS | 5.301 | 5.4093 |
| ZnSe | 5.577 | 5.6676 |
| ZnTe | 6.000 | 6.101 |
| CdS | 5.775 | 5.832 |
| CdTe | 6.420 | 6.477 |

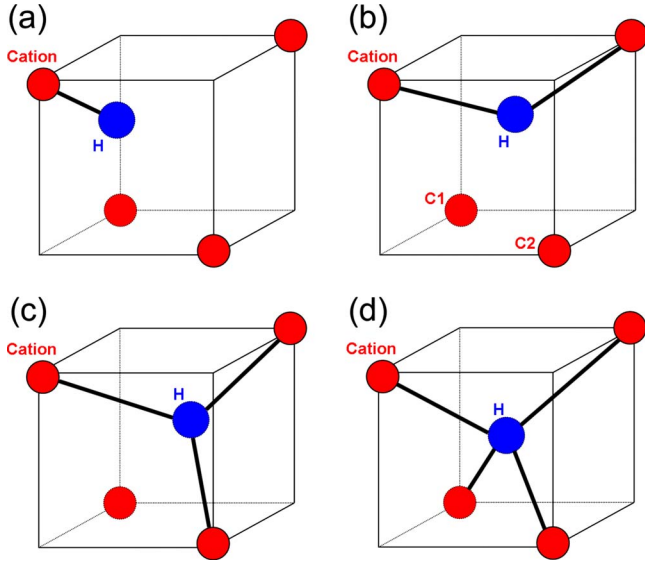


FIG. 1. (Color online) Schematic figures of hydrogen in anion vacancy ($V_{\text{anion-H}}$) with (a) onefold, (b) twofold, (c) threefold, and (d) fourfold coordinations. In (b), the atoms C1 and C2 relax away from the vacancy in the donor state, ($V_{\text{anion-H}}^+$), but move close to each other to form a cation-cation bond in the acceptor state, ($V_{\text{anion-H}}^-$).

tors listed in Table I. Figure 1 shows the schematic figures of the hydrogen in the anion vacancy with coordination number ranging from 1 to 4. We first consider the single-donor state of the $V_{\text{anion-H}}$ complex. H^- is found to be located at the center of the O vacancy in zinc-blende ZnO [see Fig. 1(d)],

consistent with the early results for wurtzite ZnO.^{4,8} When the anion is changed to S, Se, or Te, we find that H^- moves off center and is stabilized at the position with twofold coordination with Zn cations [see Fig. 1(b)]. The energies for the structures with other H coordination numbers (relative to the energy of the ground-state H structure of twofold coordination) are shown in Table II. Replacing a large anion with a much smaller one, H^- , results in reduced electronic shell repulsion between the cations and H^- . Thus, H^- naturally moves off center to enhance the Coulomb attraction between the cations and H^- . Our calculations suggest that H^- finds a balance between the Coulomb attraction and the electronic shell repulsion when it approaches two Zn atoms around the anion vacancy. The Zn-H bond length is kept at about 1.77 Å for the twofold coordinated H when the host anion changes from S, Se, to Te as shown in Table II. The similar trend has also been found for CdS and CdTe, in which the twofold coordinated H is preferred in the anion vacancies with Cd-H bond length nearly unchanged for different host anions (see Table III). The cation atoms that do not coordinate with H relax significantly away from the anion vacancy.

We have calculated the LVMs of H in the anion vacancies of various Zn- and Cd-based II-VI semiconductors. The calculated results for the twofold coordinated H compare very well with the experimental results (see Tables II and III). The calculated LVMs for three- and fourfold coordinated H are significantly lower than the experimental values due to the weaker bonding. We note that, for ZnS, the calculated LVM for onefold coordinated H (1295 cm^{-1}) is closer to the experimental value (1325 cm^{-1}) than that for the twofold coordinated H (1252 cm^{-1}). But the onefold coordinated H is metastable. Also, the trend that the measured cation-H LVM

TABLE II. Energies, Zn-H bond lengths, and the H local vibrational modes (LVMs) for ($V_{\text{anion-H}}^+$) complexes in Zn-based II-VI semiconductors in zinc-blende structure. The experimental LVMs are found in Ref. 29. The energies of various ($V_{\text{anion-H}}^+$) structures for each material are relative to that of the most stable one.

| | Coordination number | Energy (eV) | $d_{\text{Cd-H}}$ (Å) | LVM (cm^{-1}) | |
|------|---------------------|-------------|-----------------------|--------------------------|------------|
| | | | | Theory | Experiment |
| ZnO | 4 | | 2.000 | 723 | |
| ZnS | 1 | 0.17 | 1.672 | 1295 | |
| | 2 | 0 | 1.765 | 1252 | 1325 |
| | 3 | 0.16 | 2.033 | 673 | |
| | 4 | 0.34 | 2.293 | 341 | |
| ZnSe | 1 | 0.21 | 1.627 | 1447 | |
| | 2 | 0 | 1.767 | 1231 | 1315 |
| | 3 | 0.29 | 2.063 | | |
| | 4 | 0.55 | 2.365 | | |
| ZnTe | 1 | 0.18 | 1.591 | 1588 | |
| | 2 | 0 | 1.772 | 1192 | 1215 |
| | 3 | 0.48 | 2.215 | | |
| | 4 | 0.82 | 2.487 | | |

TABLE III. Energies, Cd-H bond lengths, and the local vibrational modes (LVMs) for $(V_{\text{anion}}\text{-H})^+$ complexes in Cd-based II-VI semiconductors in zinc-blende structure. The experimental LVMs are found in Ref. 29. The energies of various $(V_{\text{anion}}\text{-H})^+$ structures for each material are relative to that of the most stable one.

| | Coordination number | Energy (eV) | $d_{\text{Cd-H}}$ (Å) | LVM (cm^{-1}) | |
|------|---------------------|-------------|-----------------------|--------------------------|------------|
| | | | | Theory | Experiment |
| CdS | 1 | 0.20 | 1.836 | 1201 | |
| | 2 | 0 | 1.911 | 1228 | 1265 |
| | 3 | 0.10 | 2.137 | | |
| | 4 | 0.31 | 2.402 | | |
| CdTe | 1 | 0.26 | 1.748 | | |
| | 2 | 0 | 1.915 | 1188 | 1205 |
| | 3 | 0.36 | 2.207 | | |
| | 4 | 0.77 | 2.578 | | |

in the II-VI semiconductors decreases with increasing anion size is consistent with the calculated LVMs for the twofold coordinated H in the anion vacancies but not with the one-fold coordinated H.

The Zn-H and Cd-H bonds in the anion vacancies of II-VI semiconductors have mainly ionic character. Here we want to emphasize that the concepts of ionicity and charge transfer are extremely useful in understanding chemical bonding and the electronic structure of materials. In particular, for defects in semiconductors, the basic knowledge of chemical bonding (e.g., ionic vs covalent) is very useful for understanding defect structures and determining the charge states of defect complexes. However, the concepts of ionicity and charge transfer suffer from a certain ambiguity due to the difficulty in portioning charge in a solid. In this context, a helpful approach to analyzing charge transfer is to compare the calculated properties with what would be expected under various assumed models for charge states. To begin with we consider the density-functional charge distribution of a neutral nonspin-polarized H atom in comparison with an H^- ion.¹⁵ The charge distribution and the integral of the charge within a given radius are shown in Fig. 2. As may be seen the charge distributions and the integrals of the charge are quite different over the range shown. Considering H embedded in a solid, there will be a contribution to the density from neighboring atoms around H. However, unlike the charge density of an H or H^- s state, which is maximum at the nucleus and falls off monotonically with distance, the contribution from neighboring atoms will be largest near those atoms and will fall off approximately exponentially as one moves away from them to the location of H. Therefore one can separate out this contribution by focusing on the charge density within small spheres centered at the H site. In the present work, we analyze the charge state of H using the charge within a small sphere of radius 1.2 bohr ~ 0.635 Å. The charges contained in such a sphere are $0.37e$ and $0.51e$, for neutral H and the H^- ion (Fig. 2). For comparison, the charge integration within the sphere of radius of 1.2 bohr around H in the anion vacancy yields $0.506e$ (ZnO), $0.523e$ (ZnS), $0.521e$ (ZnSe), $0.518e$ (ZnTe), $0.504e$ (CdS), and $0.502e$ (CdTe), which are in good agreement with the result

for the H^- ion. We have also calculated the charge inside spheres of other radii for H in the S vacancy of ZnS and plotted these values in Fig. 2. As may be seen the values and the radial dependence of the charge near the H nucleus agree well with those obtained for the H^- ion, and that the charge is substantially larger than that for an H atom. One may also note a deviation above either curve for larger sphere radii. This reflects the contribution from tails of other atoms.

The four cation atoms around an anion vacancy can possibly form one or two cation-cation bonds. This was first pointed out by Chadi^{16,17} for a series II-VI and III-V semiconductors and was also discussed later by other authors.^{18–20} The consequence of cation-cation bond formation in an anion vacancy is that an anion vacancy in zinc-blende lattice can possibly take T_d (no cation-cation bond), C_{2v} (one cation-cation bond), or D_{2d} (two cation-cation bonds) symmetry. These three structures correspond to stable

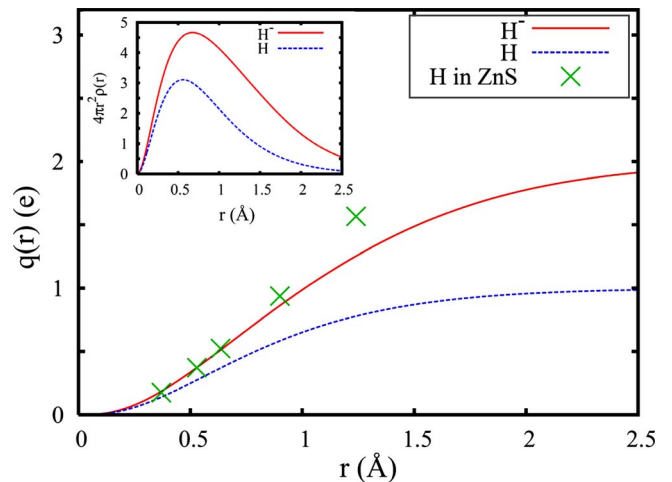


FIG. 2. (Color online) Integration of the electrons, $q(r)$, within spheres around an isolated H^- ion (solid red curve), an isolated neutral atom (dash blue curve), and H in the S vacancy of ZnS (green cross) as a function of the radius (r) of the sphere. Inset shows $4\pi r^2 \rho(r)$ as a function of r , where $\rho(r)$ is the electron density.

TABLE IV. Zn-H, Zn-Zn bond lengths, and the H local vibrational modes (LVMs) of $(V_{\text{anion}}\text{-H})^-$ complexes in Zn-based II-VI semiconductors.

| | $d_{\text{Zn-H}} (\text{\AA})$ | $d_{\text{Zn-Zn}} (\text{\AA})$ | LVM (cm^{-1}) |
|------|--------------------------------|---------------------------------|--------------------------|
| ZnS | 1.686 | 2.418 | 1620 |
| ZnSe | 1.710 | 2.423 | 1497 |
| ZnTe | 1.743 | 2.435 | 1322 |

defect charge states of +2, 0, and -2 for II-VI semiconductors and their relative stability depends on the Fermi level. This is true for most of the II-VI semiconductors except for the case with a small anion. For instance, in ZnO, the dimerization of the cations around O vacancy was not found.¹⁹ The insertion of H in the O vacancy of ZnO results in a fourfold coordinated H. In other II-VI semiconductors under this study, the insertion of H in the anion vacancy still allows the formation of one cation-cation bond but prevents the formation of the second cation-cation bond as H is coordinated with two cations.

The $V_{\text{anion}}\text{-H}$ complex in the II-VI semiconductors studied here can either be a single-electron donor or acceptor. When the Fermi level is low, H^- binds with V_{anion}^{2+} (no cation-cation bond), resulting in a single-electron donor with two cations coordinated with H^- while the other two [labeled C1 and C2 in Fig. 1(b)] relax away from the vacancy. When the Fermi level is high, H^- binds with V_{anion}^0 [one cation-cation bond between atoms C1 and C2 in Fig. 1(b)], resulting in a single-electron acceptor. In $(V_{\text{anion}}\text{-H})^-$, the accumulated electrons along the cation-cation bond repel the H^- ion, resulting in shorter cation-H bonds and higher H LVMs, as shown in Tables IV and V. $V_{\text{O}}\text{-H}$ in ZnO only exists as a donor since no Zn-Zn bond can be formed. For most of the other II-VI semiconductors with zinc-blende structure, $V_{\text{anion}}\text{-H}$ is amphoteric. Figure 3 shows the (+/-) transition level within the band gap for $V_{\text{anion}}\text{-H}$ in various II-VI semiconductors. The amphoteric behavior is also expected for these semiconductors in wurtzite structure.

Interestingly, the (+/-) transition levels for $V_{\text{anion}}\text{-H}$ in Fig. 3 are roughly lined up in absolute scale within half electron volt. The (+/-) transition level is the Fermi level at which the energies of $(V_{\text{anion}}\text{-H})^+$ and $(V_{\text{anion}}\text{-H})^-$ are equal to each other. The energy difference between $(V_{\text{anion}}\text{-H})^+$ and $(V_{\text{anion}}\text{-H})^-$ is largely determined by the energy difference between the empty cation dangling-bond orbital and the filled cation-cation bonding orbital. The Zn-Zn bond lengths for ZnS, ZnSe, and ZnTe are approximately the same as shown in Table IV, justifying the close alignment of the

TABLE V. Cd-H, Cd-Cd bond lengths, and the H local vibrational modes (LVMs) of $(V_{\text{anion}}\text{-H})^-$ complexes in Cd-based II-VI semiconductors.

| | $d_{\text{Cd-H}} (\text{\AA})$ | $d_{\text{Cd-Cd}} (\text{\AA})$ | LVM (cm^{-1}) |
|------|--------------------------------|---------------------------------|--------------------------|
| CdS | 1.845 | 2.736 | 1563 |
| CdTe | 1.888 | 2.742 | 1313 |

TABLE VI. Energies and cation-H bond lengths of $(V_{\text{anion}}\text{-F})^+$ complexes in ZnS and CdTe. The energies of various $(V_{\text{anion}}\text{-F})^+$ structures for each material are relative to that of the most stable one.

| | Coordination number | Energy (eV) | $d_{\text{cation-F}} (\text{\AA})$ |
|------|---------------------|-------------|------------------------------------|
| ZnS | 1 | 0.06 | 2.143 |
| | 2 | 0.03 | 2.048 |
| | 3 | 0 | 2.154 |
| | 4 | 0.07 | 2.316 |
| CdTe | 1 | 0.27 | 2.241 |
| | 2 | 0 | 2.186 |
| | 3 | 0.03 | 2.364 |
| | 4 | 0.28 | 2.576 |

(+/-) levels among the Zn-based compounds. In addition, the electronegativities of Zn (1.65) and Cd (1.69) are nearly same. This may explain the closeness of the (+/-) transition levels for $V_{\text{anion}}\text{-H}$ in the Zn-based and Cd-based II-VI semiconductors. The (+/-) transition levels for the interstitial H in various semiconductors and insulators have also been found to be roughly aligned.²¹ However, for the interstitial H, the (+/-) transition level is largely determined by the energy difference between the empty cation dangling-bond level and the filled anion dangling-bond level.²¹

IV. DISCUSSION

It is often useful to analyze structures of ionic compounds in terms of ionic radii.²² In particular, bond lengths in halides and ionic chalcogenides rarely deviate by more than a few percent from the values indicated by the ionic radii and, furthermore, when there are large deviations it is often indicative of interesting hybridization effects as in, e.g., Pb containing perovskites such as PbTeO_3 , where Pb-O hybridization stabilizes ferroelectricity. However, H^- is a particularly flexible ion, i.e., the variability in its bond lengths is larger than for halide anions and consistent ionic radii for H^- are therefore not tabulated.²²⁻²⁴ However, in an ionic hydride with low-electronegativity metals, H^- often behaves similarly to F^- from a structural point of view.²⁵⁻²⁷ For instance, the LiH lattice constant (4.083 \AA) is nearly the same as that for LiF (4.027 \AA).

Our calculations on the structures of H and F in the anion vacancy of ZnS and CdTe show that H and F behave similarly as anions except for different cation-H and cation-F bond lengths (see Tables II, III, and VI). In the S vacancy of ZnS, the longer Zn-F bond length results in the threefold coordinated F rather than the twofold coordinated one adopted by H. The shorter cation-H bond compared to the cation-F bond indicates some degree of hybridization between the H states and the host states.

The Zn- and Cd-based II-VI semiconductors studied here are not purely ionic materials. The Ewald field that stabilizes the H^- ion is stronger in ionic hosts and weaker in more

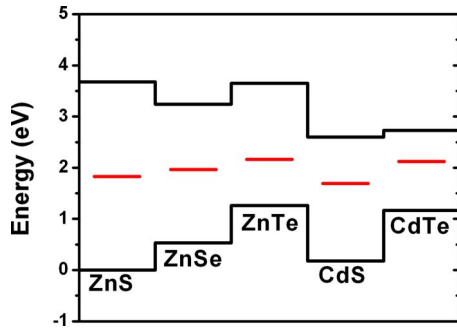


FIG. 3. (Color online) Calculated (+/-) levels for $V_{\text{anion}}\text{-H}$ complex in several II-VI semiconductors. For each semiconductor, the lower and upper black lines indicate the valence and conduction-band edges, respectively. The red line indicates the (+/-) transition level for the $V_{\text{anion}}\text{-H}$. The valence-band offset is taken from Ref. 29. The conduction-band edges are shifted to reflect to the experimental band gaps.

covalent hosts. As such, the H^- in an anion vacancy of a more covalent host will also tend to be more hybridized even if the chemical species of the nearest-neighbor cations are the same as in ZnTe in comparison with ZnO. Figure 4 shows the projected density of states (PDOS) for the hydrogen s orbital in the anion vacancies of ZnO and ZnTe. The high-energy part of the H PDOS [e.g., the PDOS peak (>5 eV) in Fig. 4(a)] is largely the H $2s$ state and its resonance with the conduction-band states. There is small H $1s$ contribution near the conduction-band edge, which is the result of the covalent type of hybridization between the filled H $1s$ and empty Zn $4s$ states. It is noticeable that the hybridization between H and the host band states in ZnTe is en-

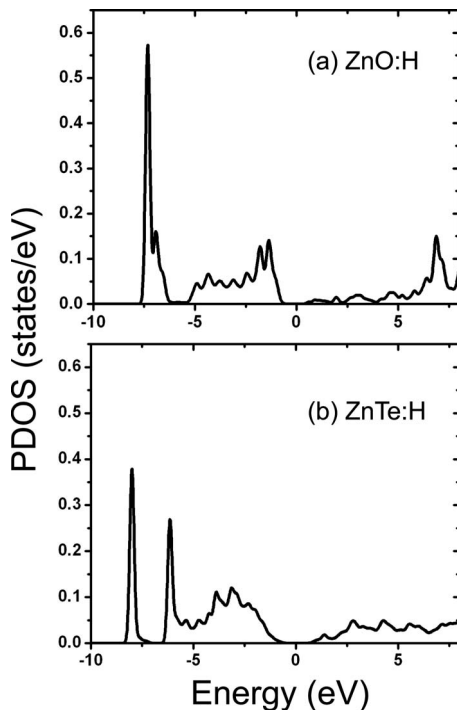


FIG. 4. Density of states projected on the s orbital of hydrogen in anion vacancies of (a) ZnO and (b) ZnTe.

hanced compared to that in ZnO because ZnTe is more covalent than ZnO and the Te states in ZnTe are much more dispersive than the O states in ZnO. Our calculations show that the maximum valence electron density near H is higher than that near Te in ZnTe but lower than that near O in ZnO, reflecting the increasing electronegativity from Te, H, to O. The fact that the Zn and Cd atoms can make cation-cation covalent bonds in the anion vacancy for the acceptor structure of $V_{\text{anion}}\text{-H}$ (except for oxides) indicates some degree of covalency in the system. In highly ionic materials, the formation of the cation-cation covalent bond is unlikely for highly electropositive cations regardless of the anion size, thereby rendering $V_{\text{anion}}\text{-H}$ only stable as a shallow donor.

We have also calculated the H structures in the As vacancy of GaAs, a more covalent semiconductor. We find that H in $(V_{\text{As}}\text{-H})^{2+}$ is onefold coordinated, forming a single covalent bond with a nearby Ga atom. Clearly, the ionicity of the host material has a critical effect on the bonding of H in the vacancy.

Finally, we want to point out that multicoordination that is incompatible with the number of available electron pairs is usually the indication of ionic bonding in compounds with cations and anions of very different electronegativities. It can also be the result of metallic bonding if the atoms in the system have similar electronegativities. In an ionic crystal or a highly polar semiconductor, it is the electronic shell repulsion that causes the multicoordination of H in anion vacancies, while the absence of such repulsion results in the absence of multicoordination for the H in cation vacancies. In a cation vacancy, H is usually a donor, H^+ . Without an electron shell, H^+ can move deeper into the electron shell of the anion atom until the Coulomb attraction is screened out. Thus, H^+ usually binds with only one anion atom in the cation vacancy such as the case for H in Cd vacancy of CdTe.²⁰ Also, the anion-H bond length is often shorter than the ionic radius of the anion.

V. CONCLUSIONS

We study the structure, the nature of bonding, and the local vibrational modes for hydrogen in anion vacancies of various Zn- and Cd-based II-VI semiconductors. Our results show that, in polar semiconductors with relatively high ionicity, hydrogen in an anion vacancy is anionic as H^- ion with multicoordination. The coordination number depends on the anion size. In all the II-VI semiconductors we have studied, i.e., ZnX ($X=\text{O}, \text{S}, \text{Se}, \text{and Te}$) and CdX ($X=\text{S and Te}$), H always takes a twofold coordinated structure in the anion vacancy except for ZnO in which H is a fourfold coordinated in the O vacancy. On the other hand, in the anion vacancies of more covalent semiconductors such as GaAs, hydrogen prefers to form a single covalent bond with a cation atom around the anion vacancy. Our results also suggest that, in the zinc-blende and wurtzite II-VI semiconductors, the $V_{\text{anion}}\text{-H}$ complex is usually amphoteric, either being a single-electron donor (H^- in V_{anion}^{2+}) or being a single-electron acceptor (H^- in neutral V_{anion} with a cation-cation bond in the vacancy). The exception occurs for the semiconductors with small anion size and high anion electronegativity, such as

ZnO and GaN, etc., in which $V_{\text{anion}}\text{-H}$ acts only as shallow donor because the anion vacancy is too small to accommodate both an H^- ion and a cation-cation bond needed for the acceptor structure.

ACKNOWLEDGMENTS

This work was supported by the U.S. DOE Office of Non-proliferation Research and Development NA22.

-
- ¹C. G. Van de Walle, Phys. Rev. Lett. **85**, 1012 (2000).
²S. Nakamura, N. Iwasa, M. Senoh, and T. Mukai, Jpn. J. Appl. Phys., Part 1 **31**, 1258 (1992).
³J. Neugebauer and C. G. Van de Walle, Phys. Rev. Lett. **75**, 4452 (1995).
⁴A. Janotti and C. G. Van de Walle, Nature Mater. **6**, 44 (2007).
⁵A. Janotti and C. G. Van de Walle, Appl. Phys. Lett. **92**, 032104 (2008).
⁶A. K. Singh, A. Janotti, M. Scheffler, and C. G. Van de Walle, Phys. Rev. Lett. **101**, 055502 (2008).
⁷C. G. Van de Walle, Phys. Rev. B **56**, R10020 (1997).
⁸H. Takenaka and D. J. Singh, Phys. Rev. B **75**, 241102(R) (2007).
⁹W. Martienssen, Z. Phys. **131**, 488 (1952).
¹⁰S. S. Mitra and Y. Brada, Phys. Rev. **145**, 626 (1966).
¹¹G. A. Tanton, R. A. Shatas, R. S. Singh, and S. S. Mitra, J. Chem. Phys. **52**, 538 (1970).
¹²G. Kresse and J. Furthmüller, Phys. Rev. B **54**, 11169 (1996).
¹³G. Kresse and D. Joubert, Phys. Rev. B **59**, 1758 (1999).
¹⁴M.-H. Du, H. Takenaka, and D. J. Singh, Phys. Rev. B **77**, 094122 (2008).
¹⁵ H^- ion is stabilized by a Watson sphere [R. W. Watson, Phys. Rev. **111**, 1108 (1958)] of radius of 3.06 bohr. The charge integration within a small sphere, e.g., 1.2 bohr, is not sensitive to the choice of the radius of Watson sphere.
- ¹⁶D. J. Chadi, Mater. Sci. Forum **258-263**, 1321 (1997).
¹⁷D. J. Chadi, Mater. Sci. Semicond. Process. **6**, 281 (2003).
¹⁸S. Lany and A. Zunger, Phys. Rev. Lett. **93**, 156404 (2004).
¹⁹S. Lany and A. Zunger, Phys. Rev. B **72**, 035215 (2005).
²⁰M.-H. Du, H. Takenaka, and D. J. Singh, J. Appl. Phys. **104**, 093521 (2008).
²¹C. G. Van de Walle and J. Neugebauer, Nature (London) **423**, 626 (2003).
²²R. D. Shannon, Acta Crystallogr., Sect. A: Cryst. Phys., Diffraction, Theor. Gen. Crystallogr. **32**, 751 (1976).
²³D. F. C. Morris and G. L. Reed, J. Inorg. Nucl. Chem. **27**, 1715 (1965).
²⁴L. Pauling, Acta Crystallogr., Sect. B: Struct. Crystallogr. Cryst. Chem. **34**, 746 (1978).
²⁵C. E. Messer, J. Solid State Chem. **2**, 144 (1970).
²⁶K. Yvon, Chimia **52**, 613 (1998).
²⁷F. Gingl, L. Gelato, and K. Yvon, J. Alloys Compd. **253-254**, 286 (1997).
²⁸*CRC Handbook of Chemistry and Physics*, 88th ed., edited by D. R. Lide (Taylor and Francis, London, 2008).
²⁹J. Tatarkiewicz, M. Cardona, A. Breitschwerdt, C.-T. Lin, R. Grotzschel, and W. Witthuhn, Phys. Status. Solidi B **155**, 77 (1989).